Molecular dynamics of LiF melting

A. B. Belonoshko, R. Ahuja, and B. Johansson
Condensed Matter Theory Group, Department of Physics, Uppsala University, Box 530, S-751 21 Uppsala, Sweden
(Received 6 October 1999)

We performed molecular-dynamics simulations of the melting and/or freezing of LiF. The simulations were done using the Tosi-Fumi model and our own model of interatomic interactions. The latter was verified by *ab initio* calculations of the equation of state for LiF. We show that the recent molecular-dynamics calculations by Boehler and co-workers are not adequate and their model for the interactions is not capable of providing melting temperatures in agreement with experiment. Our calculated pressure dependence of the melting temperatures gives valuable information. We found that the $B1$-$B2$ transition in LiF at around 1 Mbar removes the discrepancy between the diamond-anvil cell and shockwave melting temperatures. An explanation of the controversy between ''low'' and ''high'' melting temperatures obtained from diamond-anvil cell experiments is suggested.

I. INTRODUCTION

Studies of materials subjected to high pressure have a twofold value, since they often contain both applied and fundamental aspects. High pressure allows us to probe such interatomic distances which, even though they occur in nature, are in regions not accessible for direct observations. This also provides a stringent test of theories of condensed matter, which, in turn, stimulate further research in high-pressure experiment.

There are two major ways to achieve high pressure—shock and diamond-anvil cell experiments. While processes in shock experiments are extremely fast, the diamond-anvil cell (DAC) technique can be used to observe material for a sufficiently long time to derive meaningful measurements. Despite the great progress in DAC technique in the past two decades, there exists a number of controversies about the results from different groups performing DAC experiments and also often significant differences between results of DAC and shock experiments.[1]

The paper in Ref. 2 reports new DAC measurements for LiF and NaCl up to 1 Mbar. The authors[2] also perform molecular-dynamics (MD) simulations of LiF melting and find the MD results in ''excellent agreement'' with DAC experiment. They also calculated that molten LiF retains the simple-cubic $B1$-like structure. Their extrapolated melting temperatures of LiF are much lower than that obtained from shock-wave experiments.

In this paper, we calculated the LiF melting curve using the MD method. We performed different kinds of simulations with two slightly different interatomic potentials. We show that the results of the MD simulations in Ref. 2 are incorrect and our calculated MD melting curve with the interatomic potential of Ref. 2 is different from what they obtained. This also means that the true melting temperature derived from their model disagrees with DAC experiment, as well as with the experimental melting temperatures at low pressures. We also show that the method which the authors of Ref. 2 applied for their calculations, referring to the experience of other researchers,[3] is not adequate and gives uncertain results. Further, we show that there is a possibility for a $B1$-$B2$ transition in LiF at about 1.3 Mbar which might make the results of DAC and shock experiments consistent with each other. We compare DAC results for the NaCl melting curve and show that they are in agreement with our previous MD simulations. We suggest an explanation which might solve the controversy between the high and low iron melting temperatures as well as the controversy between DAC low and MD high MgO melting temperatures.

The paper is organized as follows. First, we explain the two models for the interatomic interaction which have been used in our MD simulations. Further, some technical details of our MD simulations are also provided. Second, the correct melting temperature for LiF (for a given model of the interatomic interaction) is calculated and the structure of the liquid and solid LiF at the melting temperature is compared along the melting curve. Finally, we compare and discuss previous MD simulations and DAC experiments for NaCl and MgO together with presented MD LiF melting curve and suggest a mechanism which is (possibly) important to take into account while performing DAC experiments.

II. INTERATOMIC POTENTIALS

The paper by Boehler *et al.*[2] is somewhat ambiguous as regards the model which was used to represent LiF. The paper says that ''the Tosi-Fumi model [20] was employed for the interion potentials using the functional form and parameters listed by Lewis *et al.* [21].'' However, unfortunately Lewis *et al.*[4] did not list parameters for LiF. Still, Lewis *et al.*[4] lists the sources for the parameters of potentials for a number of other alkali halides. In our attempts[5] to trace an appropriate potential for LiF, the parameters listed by Sangster and Dixon[6] were accepted in our simulation to reproduce the data calculated by Boehler *et al.*[2] The subsequent comparison of our and previous[2] MD simulations (see below) confirmed that we used the same interatomic potential.

The potential employs pairwise additive interatomic terms of the forms

TABLE I. Parameters of the Tosi-Fumi potential [Eq. (1)] ($Z_{Li}=1, Z_F=-1$) for LiF.

Source	A (kJ/mole)	B ($Å^{-1}$)	C (kJ/mole $Å^6$)	D (kJ/mole $Å^8$)
Li-Li	9545.7	3.3445	4.4	1.81
Li-F	22093.3	3.3445	48.2	36.1
F-F	40569.2	3.3445	873.2	1023.7

$$V(r_{ij})=\frac{Z_iZ_je^2}{r_{ij}}-\frac{C_{ij}}{r_{ij}^6}-\frac{D_{ij}}{r_{ij}^8}+A_{ij}\exp(-B_{ij}r_{ij}), \quad (1)$$

where the individual terms represent Coulomb, van der Waals (dipole-dipole and dipole-quadrupole terms), and repulsion energy, respectively. Here r_{ij} is the interatomic distance between atoms i and j, Z is a formal charge, e is the electron charge, C_{ij} and D_{ij} are van der Waals constants, and A_{ij} and B_{ij} are parameters for the repulsive interactions. The parameters are listed in the Table I.

The performance of these potentials are rather good for describing properties of alkali halides. However, the Li salts are an exception. Their cohesive energies and lattice constants, calculated with Eq. (1), compares poorly with the corresponding experimental values. For example, LiI at room temperature is not stable and transforms into a liquidlike structure.[4] Substantial work has been done to develop better models of the interactions. Nevertheless, the quality of the models for Li salts have remained essentially the same.[7] Moreover, from the MD simulations with this potential we discovered that the potential is not applicable at high pressure. At pressures exceeding approximately 1.4 Mbar at room temperature we observed a collapse of the Li and F atoms. At high temperatures the collapse occurred at even lower pressures. This is quite understandable for the potential contains terms inversely proportional to r_{ij} in sixth and eighth degrees. At a high compression when distances becomes shorter, the van der Waals terms becomes unphysically large. This leads to a maxima at the energy-distance curve (Fig. 1). If the distance between two atoms becomes shorter than the position of the maxima, the atoms attract each other instead of a repulsion. This leads to a collapse. This is a rather common problem with this kind of potential.[8,9]

To solve this problem we decided to develop a potential which would have the following features. First, it should be applicable at any compression. Second, it should differ from the Tosi-Fumi[10] potential [Eq. (1)] as little as possible. Third, it should provide correct energies at very high compression. Therefore, the form of the new potential was chosen exactly as the Tosi-Fumi potential. However, the dipole-dipole and dipole-quadrupole interactions were set equal to zero. This is justified for LiF by the analysis provided by Dekker.[11] According to his analysis, the energy of van der Waals interactions accounts for less than 2% of the cohesion energy and their share in the energy dramatically decreases with compression. Setting all van der Waals coeeficients equal to zero and keeping the Li-Li and F-F parameters as given by Tosi-Fumi, we adjusted A_{LiF} and B_{LiF}. These parameters were fitted using the computer code GULP (Ref. 12) to reproduce

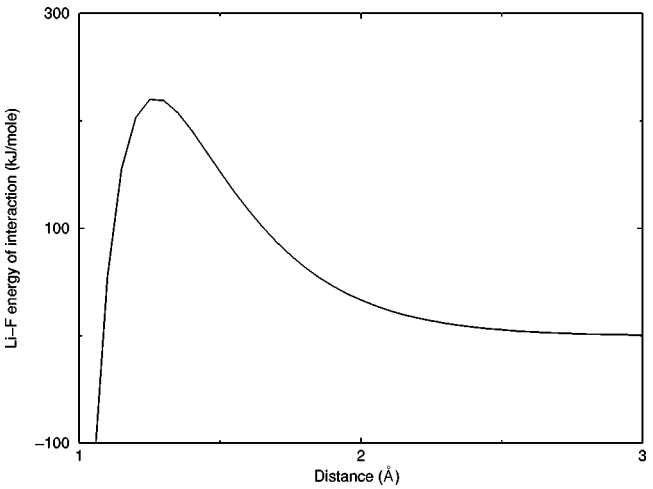

FIG. 1. The energy of interaction between Li and F atoms as a function of distance between them. The energy calculated using Eq. (1) with the parameters from Table I. The Coulomb term was not taken into account, because of its long-range character. The inclusion of the Coulomb term would shift the position of the maximum to a larger distance. The equilibrium Li-F distance in the $B1$ lattice is 2.012 Å.

the cohesion energy, the static dielectric constant,[11] and the PVT data.[13] Instead of the values for A_{LiF} and B_{LiF} given in the Table I, we calculated $A_{LiF}=38722$ kJ/mole and $B_{LiF}=3.69$ $Å^{-1}$. The potential with parameters as provided in Table I will be referred to as IP1 (interaction potential number 1). The potential of the same form [Eq. (1)], but where C and D set equal to zero and A_{LiF} and B_{LiF} are chosen as above, will be referred to as IP2.

It is obvious that IP2 does not have a maximum as IP1 does, because an exponential function (repulsive term) increases faster than r^{-1} (Coulomb term) decreases. Because we want to use IP2 at extreme pressures we should be convinced that IP2 provides reasonable values at high compression. Since experimental data[13,14] are not available above 300 kbar, we calculated the LiF 0 K isotherm from first principles.

In order to calculate the 0 K isotherm of LiF we have used the full-potential linear muffin-tin-orbital (FPLMTO) method.[15] The calculations were based on the local-density approximation and we used the Hedin-Lundqvist[16] parametrization for the exchange and correlation potential. Basis functions, electron densities, and potentials were calculated without any geometrical approximation.[15] These quantities were expanded in combinations of spherical harmonic functions (with a cutoff $l_{max}=8$) inside nonoverlapping spheres surrounding the atomic sites (muffin-tin spheres) and in a Fourier series in the interstitial region. The muffin-tin sphere occupied approximately 50% of the unit cell. The radial basis functions within the muffin-tin spheres are linear combinations of radial wave functions and their energy derivatives, computed at energies appropriate to their site and principal as well as orbital atomic quantum numbers. Outside the spheres the basis functions are combinations of Neuman or Hankel functions.[17,18] In the calculations reported here, we made use of pseudocore $1s$ states and valence band $2s$, $2p$, and $3d$ basis functions for Li and F with corresponding two sets of energy parameters, one appropriate for the semicore

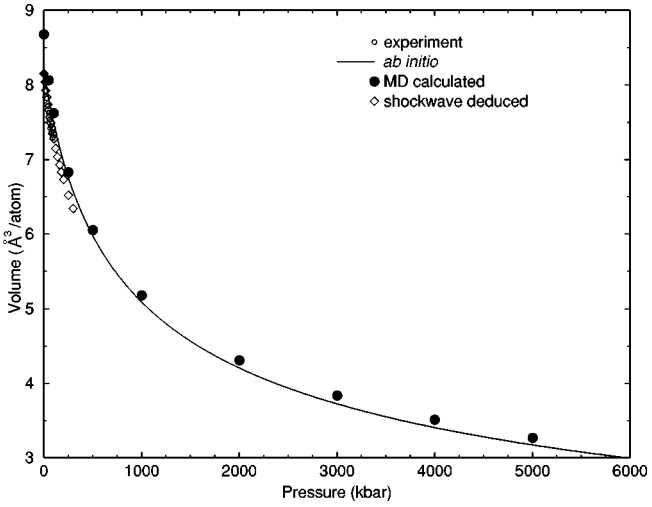

FIG. 2. The FPLMTO 0 K and MD 300 K calculated isotherms compared with experimental data. (Ref. 13,14) The data by Yagi (Ref. 13) is the result of experiment performed using a large volume high-pressure device. The data by Carter (Ref. 14) is the result of shock-wave experiments up to 1000 kbar. Thermal correction using the Mie-Gruneisen equation was applied and the 300 K isotherm up to 300 kbar was calculated.

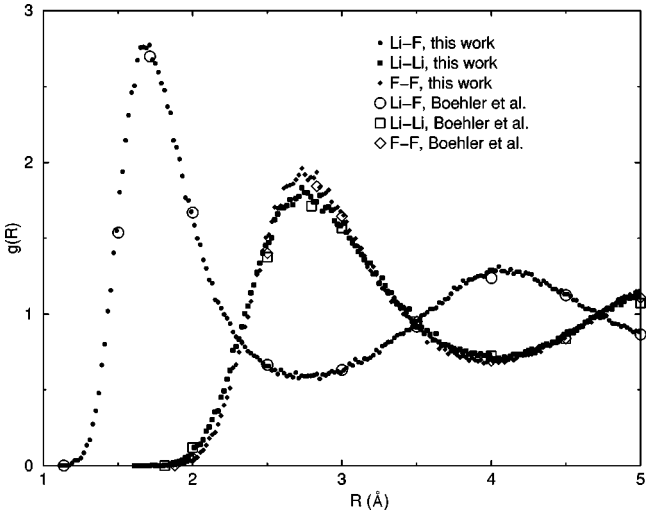

FIG. 3. Radial distribution functions $g(r)$, calculated for LiF at a temperature of 1750 K and a pressure of 100 kbar and compared with the $g(r)$, calculated by Boehler *et al.* (Ref. 2).

1*s* states, and the other appropriate for the valence states. The resulting basis formed a single, fully hybridizing basis set. For sampling the irreducible wedge of the Brillouin zone we used the special *k*-point method.[19] In order to speed up the convergence we have associated each calculated eigenvalue with a Gaussian broadening of width 20 mRy.

Figure 2 shows the FPLMTO and MD calculated isotherms of LiF with $B1$ structure compared with experimental data. The MD calculated isotherms using IP2 model volume at zero pressure is somewhat larger than both the FPLMTO and experimental volumes. Nevertheless, the pressure trend of the MD calculated volumes at 300 K is remarkably similar to the FPLMTO 0 K isotherm and there is a good agreement between experiment and calculations. Therefore, the IP2 model is applicable at high pressures.

III. MOLECULAR-DYNAMICS SIMULATION

A. Technical details

A description of the molecular-dynamics method can be found elsewhere.[20] Most of the simulations were performed using the package DL_POLY version 2.0.[21] To ensure the reliability of our results, some of the simulations were duplicated using our MD code and no relevant difference was found. Simulations in NTP (constant N is the number of particles, T is the temperature, and P is pressure) ensemble[22] were performed. The results of MD simulations in the NTP ensemble with the chosen model of the interatomic interaction depend on, apart from the initial arrangement of atoms, the number of time steps ($n_{\text{timesteps}}$), size of timestep (Δt), number of atoms (N), cutoff (r_{cutoff}) of the interatomic potential, specified time constants for temperature (τ_T), and pressure (τ_P) fluctuations. Therefore, the influence of these parameters was carefully studied by carrying out test runs at various T and P. It was found that correct results can normally be obtained with $n_{\text{timesteps}}=10\,000$, $\Delta t=0.002$ psec, $r_{\text{cutoff}}=6$ Å, $\tau_T=0.2$ psec, and $\tau_P=0.5$ psec. Still, whenever we suspected that the results might have been affected by the choice of the above parameters we varied them to be convinced that the final results are correct. The number of particles N was varied from 108 to 4096. Most of our calculations which were used for determining properties of the $B1$, $B2$, and liquid phases as well as simulations of melting and freezing were done with 4096 atoms. The long-range Coulomb energy was calculated using Ewald method[23] with the precision of 10^{-5}.

These values were normally used unless it was specifically intended to study the behavior of, for example, a small system. The assumption of a mean-field distribution of the density was applied for calculations of energy and forces at $r>r_{\text{cutoff}}=6$ Å.

B. Comparison with previous MD simulations

Boehler *et al.*[2] calculated the radial distribution functions (RDF) for each pair of Li and F atoms at the temperature of 1750 K and pressure of 100 kbar (the P and T were taken from Fig. 2 in their paper, because no tabulated data was provided, therefore the value of T can be subjected to some error). The RDF $g_{ij}(R)$ is a density of probability to find atom j at the distance R from atom i.[20] Even though we were confident that the IP1 model is what was used by Boehler *et al.*,[2] we decided to carry out an MD run at exactly the same T and P with the same number of particles ($N=216$) as was done by the authors.[2] The initial configuration of atoms was the $B1$ lattice with 108 Li and 108 F atoms. Figure 3 shows a comparison between our and earlier[2] calculated RDF's. As one can see, the agreement is perfect, especially taking into account the error of digitizing Fig. 3 given by Boehler *et al.*[2] and the fact that Boehler *et al.* did not provide the exact value of the temperature for this particular calculation. Therefore, we became convinced that the IP1 model was the model which was used by Boehler and co-workers in their MD calculations.

By carefully examining the MD calculations done by Boehler and co-workers, we found them to be incorrect. There are several reasons for this. In what follows we will analyze these reasons.

(a) Calculation of a thermal instability temperature instead of melting temperature.

The authors[2] used the so-called ''heat-until-it-melts'' method for calculating melting temperatures of LiF at a given pressure. The method gives the temperature of a thermal instability instead of a melting temperature. Referring to the experience of other researchers[3] the precision of the calculations was estimated as ± 100 K. This experience was demonstrated to be wrong in a number of papers.[8,24–28] The method chosen by the authors[2] of Ref. 2 always gives temperatures higher than the real melting temperatures. The difference between thermal instability and melting temperatures increases with pressure. It can, in fact, be very large, and, as will be shown below, amounts to about 1500 K at the pressure of 1 Mbar.

(b) Comparably small number of particles.

The authors[2] of Ref. 2 have chosen to work with a system with 216 atoms. Earlier work on MgO (Ref. 3) had demonstrated that a MD calculation of the temperature of the thermal instability (not melting) requires 1000 or more atoms.

(c) The model is not adequate.

As was briefly mentioned above, Li salts are known to be poorly modeled by the IP1 model. For example, the temperature of the thermal instability of LiF at a pressure of 1 bar calculated with 216 atoms is slightly above 600 K. The measured melting temperature of LiF at a pressure of 1 bar is 1121 K. Since the thermal instability temperature has to be higher than the melting temperature for the same model of interatomic interaction, it is clear that the mismatch is larger than at least 500 K.

(d) The IP1 model cannot be applied at high pressure.

The authors[2] provided one of the MD ''melting'' points at 2.7 Mbar and 4000 K. As we showed (Fig. 1) the IP1 gives rise to unphysical behavior at short distances, which is equivalent to high pressures. From a comparison between Figs. 1 and 3 (the RDF in Fig. 3 was calculated at a pressure of 100 kbar and a temperature of 1750 K) one can see that the distances between the Li and F atoms (Fig. 3) are already comparable with the position of Li-F energy maxima (Fig. 1). Since higher pressure and temperature makes this distance even smaller in the liquid state, the point at 2.7 Mbar and 4000 K simply could not be calculated (in fact, as we checked, even considerably lower pressures are not accessible with the IP1 model). Possibly, the collapse of the Li-F atoms was erroneously attributed to thermal instability in Ref. 2.

(e) The relative stability of the $B1$ and $B2$ phases was not checked.

Alkali halides are known to undergo a structural transition from $B1$ to $B2$ structure. Such a transition causes a drastic change of the melting curve.[24] Therefore, to provide any meaningful extrapolation of the melting of alkali halides the possibility of a $B1$-$B2$ transition must be considered.

We will provide more details justifying the above points below.

To check the possibility that for some reason our calculations are in error, we calculated the diffusion coefficients of Li and F at the same conditions as was done by Ciccotti *et al.*[29] and obtained very close agreement. We, Ciccotti *et al.*,[29] and Boehler *et al.*[2] used the same (IP1) model. Therefore, we are confident that our calculations are correct.

C. Melting versus thermal instability

There is a widespread confusion that one can calculate the temperature for the thermal instability and this temperature can be thought of as a good approximation of the melting temperature. Possibly, this confusion comes from the observation that at low pressures the difference is not that large. Indeed, as was calculated[26,27] for the melting of Al_2O_3, the difference between these two temperatures is about 200 K at room pressure and this constitutes about 10% of melting temperature. The difference is already sizeable but still can be tolerated for making certain conclusions. However, the difference increases with pressure, following the behavior of enthalpy of melting. At a pressure of 1 Mbar the difference amounts to about 1000 K.

The method for calculating the thermal instability is straightforward. One takes a crystal configuration of a certain number of atoms. Let us say we want to calculate the thermal instability temperature at some given pressure. Each subsequent MD run is carried out at this pressure and at higher T than the previous one. The new runs at increasing T are carried out until one observes a sudden change of volume, diffusion, structure, etc. The value of T where it happens is the T for the thermal instability. The precision of T for the thermal instability is defined by the used increment of T. Below we will call this method ''heat-until-it-melts'' or the one-phase simulation method.

The thermodynamically justified approach to calculating melting temperature consists in calculating Gibbs free energies of solid and liquid phases and determining the T at certain P where these two energies are equal. However, the direct calculations of Gibbs free energies from MD simulations have some drawbacks.[30] It was found that the so-called two-phase simulation method provides practically the same melting temperatures as the calculation of the Gibbs free energies.[30] We have now obtained considerable experience with this method[8,24–28] and we have found that the two-phase simulation method is a simple and efficient way to simulate (note the difference between ''calculate'' and ''simulate'') the freezing and/or melting transition. In the two-phase simulation one uses an initial configuration which consists of a solid and a liquid part. Carrying out MD simulations with that initial configuration at a certain P and T, one can easily conclude about the stability of the liquid and/or solid phase by analyzing the resulting configuration. This method was described in detail by Belonoshko *et al.* in Ref. 24.

The initial configuration for simulation of melting was prepared in the following manner. First, the $B1$ lattice was generated by translating the unit cell 8 times in the x,y, and z directions. Second, the MD run with half of the atoms as frozen was carried out at $T=2500$ K and $P=1$ bar. As a result a supercell which contained a crystal and a liquid phase with a common interface was obtained. This supercell was then used as the initial configuration for further simulations of melting and solidification in the NTP ensemble. The melting of LiF with $B2$ structure was simulated in a similar

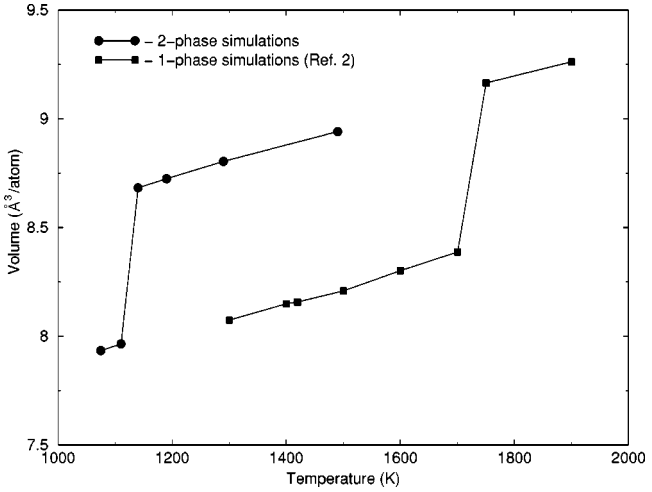

FIG. 4. MD calculated volumes of LiF at 100 kbar and for a number of temperatures using the IP1 model and two different methods, (a) ''heat-until-it-melts'' (one-phase simulation with 216 atoms) and (b) initial configuration with solid-liquid interface (two-phase simulation with 4096 atoms). The discontinous change of volume is a sign of a transition from solid to liquid (as also confirmed by detailed analysis). Two-phase simulations provide correct melting temperature, while the one-phase simulation gives an incorrect ''melting'' temperature.

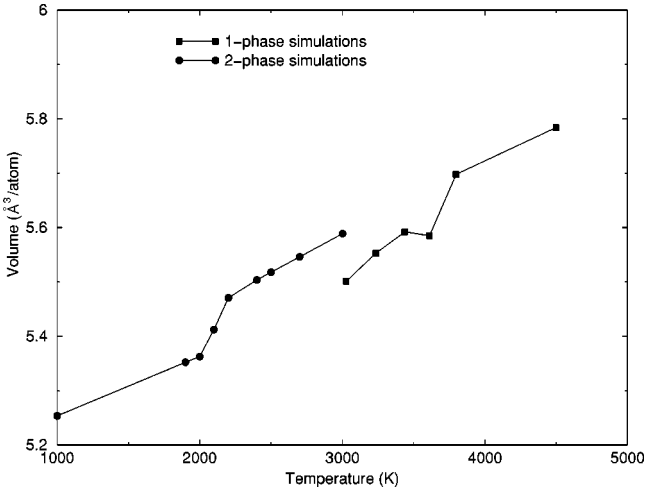

FIG. 5. MD calculated volumes for LiF at 1000 kbar and various temperatures using the IP2 model and one-phase and two-phase simulation methods. Both curves are calculated for 4096 atoms. The difference between the melting temperature and the temperature of thermal instability is about 1500 K.

manner with the only difference that instead of the initial $B1$ lattice the $B2$ lattice was generated.

Figure 4 illustrates the importance of using the correct method for calculation of the melting temperature and the importance of using a large number of particles. The correct method with a large number of particles (4096) gives a melting temperature (1140 K) which is about 600 K less than the temperature for the thermal instability calculated with a small number of particles (216). Note, that we used the same model (IP1) as was used by Boehler *et al.*[2] They calculated a melting temperature of approximately 1750 K at this pressure (100 kbar).

The importance of using a correct method to derive the melting temperature is further illustrated in Fig. 5. This figure shows the volumes, calculated using two methods at the pressure of 1000 kbar with the IP2 model and a supercell of 4096 atoms. Since the IP2 and IP1 models are very much alike we can expect a similar difference in the positions for the abrupt volume changes for the IP1 model as well. The abrupt change of volume, which is an indication of the solid-liquid transition, happens at quite different temperature, namely, about 2100 K (true melting temperature) and about 3700 K (temperature of thermal instability). The difference is huge. If we would use a small number of particles the difference would be even larger.

We can conclude this section by emphasizing that melting and thermal instability should never be considered as phenomena which occur at temperatures close to each other. Especially it is dangerous when a small number of atoms is used in the simulation. A mixing of these two phenomena might lead to quite erroneous conclusions.

D. LiF melting curve

The melting and/or freezing was simulated as described above using the IP2 model and the two-phase simulation method with 4096 atoms in the simulation cell. The phase transition was detected by a discontinous change of the volume and the diffusion coefficient, the structure and the animation of the time history of the atomic positions. Since the model itself, which is closely related to the Tosi-Fumi model, does not provide a melting temperature in agreement with experimental data at low pressure, we cannot rely on the absolute values of the calculated melting temperatures at high pressures. Nevertheless, the pressure dependence of the melting is of value, because the IP2 model is consistent with the high-pressure data (see Fig. 2).

The calculated melting curve (Fig. 6) has a high gradient at low pressure and rather quickly flattens with increasing

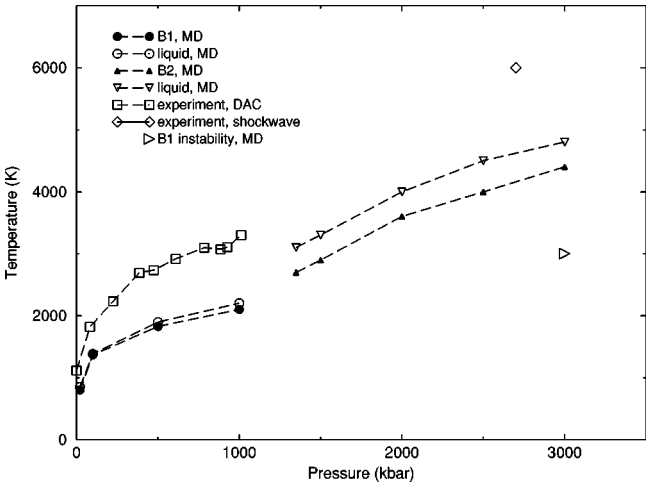

FIG. 6. MD calculated points of stability for the solid (filled symbols) and liquid (open symbols) compared with experimental DAC (Ref. 2) and shock-wave (Ref. 32) data. The right-hand open triangle at 3000 kbar shows the point where the final product of the simulation was liquid, when the solid part of a two-phase computational cell was LiF with B1 structure. This gives additional confirmation that this is indeed the field of stability for the B2 structure.

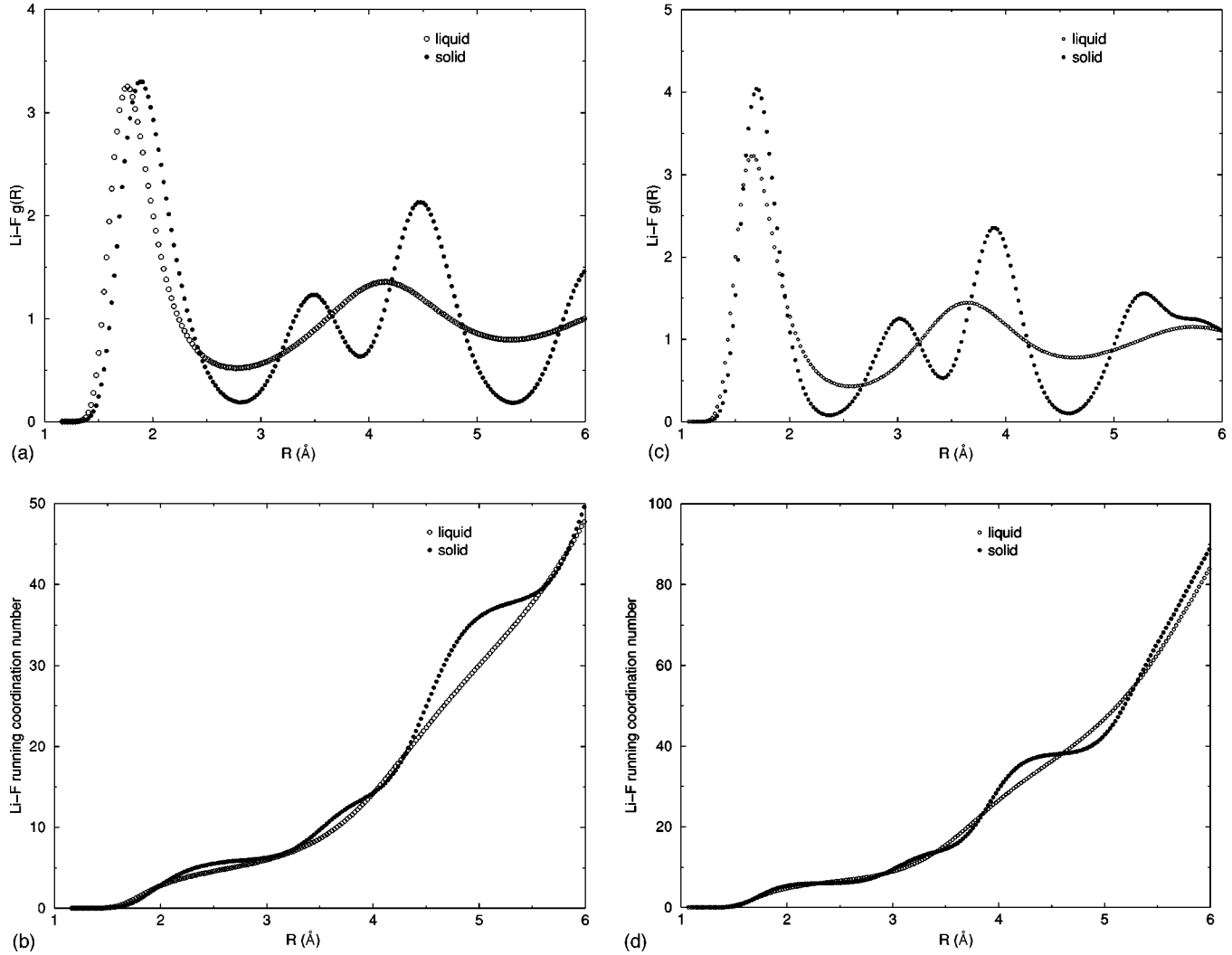

FIG. 7. Li-F radial distribution function (RDF) $g(r)$ and the corresponding running coordination number (RCN) in solid (B1) and liquid LiF along the melting curve at 100 kbar and 1385 K (a,b) and at 1000 kbar and 2200 K (c,d).

pressure in accord with experimental data. At a pressure of 1 Mbar the difference between experiment[2] and calculations is about 1000 K. At pressures above 1 Mbar the $B2$ phase melts at a higher temperature than the $B1$ phase does. It means that at this pressure we have a triple ($B1$-$B2$-liquid) point. In fact, there is some indication in the experimental data (Fig. 6) which points to the possibility of a $B1$-$B2$ phase transition (note the experimental melting point at the highest pressure). The possibility of a $B1$-$B2$ transition at a pressure above 900 kbar was suggested by Carter.[14] This was made on the observation that the velocity of shock-wave propagation in LiF has some irregular behavior above that pressure. The transition pressure can also be estimated to be close to 1 Mbar on the basis of recent ab initio calculations.[31] The $B1$-$B2$ transition can account for the discrepancy between DAC (Ref. 2) and shock-wave[32] measurements. The difference between the MD melting curve and the shock-wave melting point is about 1000-K. Because this is about the difference between the MD melting curve and the DAC melting curve at 1-Mbar, we can conclude that the $B1$-$B2$ transition is sufficient to get an agreement between the two sources of experimental data.

E. Structure of LiF along melting curve

In Ref. 2 it is stated that ''molecular-dynamics simulations predict that molten LiF retains a simple-cubic $B1$-like structure.'' The authors also state that the structure of solid and liquid LiF are very much alike close to melting. Possibly, when the structure of the fluid and the structure of overheated metastable solid LiF are compared, one can come to that conclusion. However, Fig. 7(a) shows a comparison between the Li-F radial distribution function (RDF) in the solid ($B1$) and in the liquid phase at 100 kbar and 1385 K. As one can see, the difference between the structures is quite evident. The running coordination number (RCN) [Fig. 7(b)] at this pressure is about four, which suggests a tetrahedral coordination of the Li ion. We observe essentially the same change of structure at 1000 kbar and 2200 K—the highest calculated PT melting point of LiF with the $B1$ structure. However, the RCN in the liquid is close to 6 (as in solid $B1$). Probably, this convergence of RCN in the liquid and the solid at melting with increasing pressure suggested the conclusion[2] in Ref. 2 about the similarity of the liquid and solid structures at high pressure. We should point out that the convergence of RCN is the only similarity. The structures of

the liquid and the solid remain quite distinct—with long-range order and nonmixing high-order neighbor shells in the solid.

IV. DISCUSSION

Since the calculated melting temperatures of LiF are substantially lower than the experimental ones at low pressure, we cannot rely on their calculated absolute values at high pressure. Nevertheless, because the room-temperature isotherm of LiF (Fig. 2) was calculated to be in good agreement with the experimental data and our first-principles calculation, it is possible that the pressure dependence of the melting temperature is close to the experimental behavior. Indeed, the LiF MD melting curve and the experimental DAC LiF melting curve[2] exhibit common features—a rapid increase of the melting temperature at low pressure and a considerable flattening of the curve at high pressures. The recent paper in Ref. 2 also presented new experimental data on the NaCl melting up to 1 Mbar. Melting of NaCl was previously simulated[24] using the MD method. It is, of course, interesting to compare these two curves. The NaCl MD melting curve is close to the measured one. However, here we can discuss also the absolute values of the temperature because the low-pressure experimental melting temperature[33] was reproduced almost exactly both in our MD study[24] and in the experiment in Ref. 2. It is interesting to see that when $B1$ (at 0 pressure) and $B2$ (at about 300 kbar) become stable, we have nearly perfect agreement between theory and experiment. However, with further increase of pressure the theoretical curve goes above the experimental one, even though the difference is almost within the experimental errors. The agreement between the two curves is quite remarkable, because the curve was *predicted*, therefore, there is no way that the experiment could affect our way of modeling.

MD simulations provide us with a very detailed picture of the melting mechanism which gives us insight into the reason for the flattening of the melting curves as a function of pressure. If there is no solid-solid phase transition the structure of the solid remains of course unchanged. This can be different for the liquid phase. The coordination number in the liquid increases with pressure and becomes close to that in the solid. Because at high pressure most of the configurational energy comes from the nearest neighbors, the compressibility of the two phases becomes increasingly similar. This leads to small volume changes at melting. Due to the fact that the solid remains long-range ordered, i.e., opposite to the liquid phase, the pressure dependence of the entropy change associated with the melting is comparably weak. As a result, the slope of the melting curve becomes smaller with increasing pressure. We should emphasize, however, that the effect has no direct connection with temperature. It is only the pressure which makes the melting curve flat. In this regard the comparison (Fig. 8) of MgO MD and DAC melting curves makes us wonder if the DAC experiment indeed measured melting temperatures and not something else. While the MD MgO melting curve exhibit common features with the melting curves for LiF and NaCl (both theoretical and experimental) showing a rapid increase of the melting temperature at low pressure and a flattening at high pressure, the DAC MgO melting curve constitutes an exception. The gradient of the DAC MgO melting curve is extraordinary low. The melting temperature was determined by (1) the discontinuous change in the absorption of the laser radiation and (2) by the observation of surface motion.[2] This method works excellently at low pressure, and we can therefore pose the question: ''Is it possible that the surface motion (which obviously also will cause a change of the absorption) is a manifestation of melting at low pressure and a manifestation of something else at high pressure?'' The answer is yes, it is possible. This has already been demonstrated in our earlier paper.[34] Here we suggest a simplified explanation which should be considered as merely a hypothesis yet to be confirmed or rejected by further experimental studies. Our explanation is illustrated by Fig. 9.

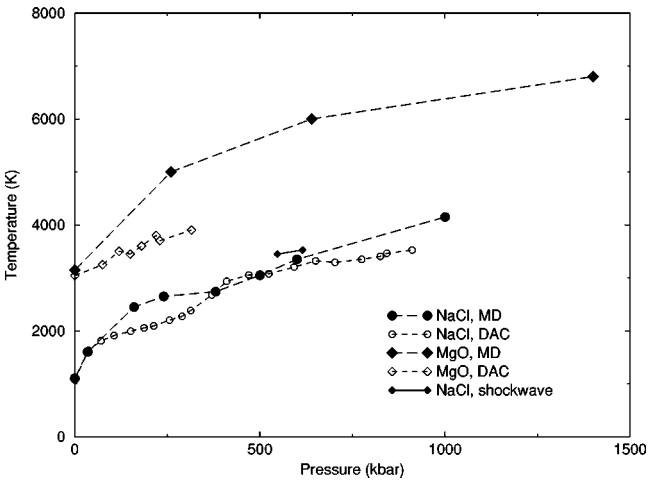

FIG. 8. MD predicted melting curves of MgO and NaCl (Ref. 24) compared with shock-wave (Ref. 37) and recent DAC data for MgO (Ref. 38) and NaCl (Ref. 2).

A sample in DAC is subjected to thermal stress which increases with temperature, because the sample is heated in-

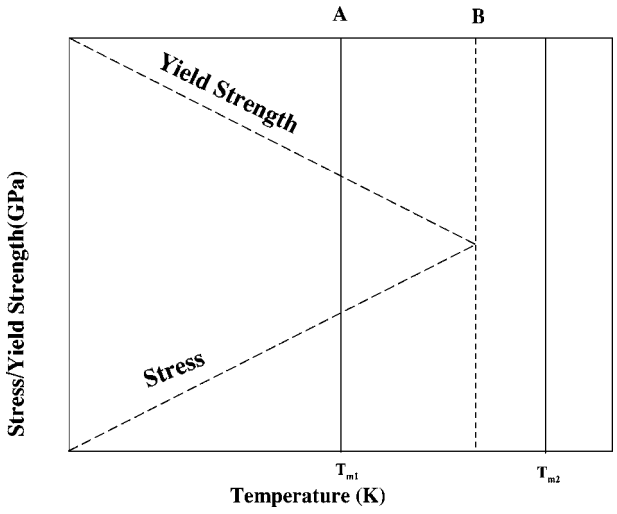

FIG. 9. A schematic illustration of two possible scenarios when measuring melting temperatures in a diamond-anvil cell. Melting temperature is low (T_{m_1}) and the thermal stress curve and yielding limit curve do not cross before melting (scenario A). Melting temperature is high (T_{m_2}) and the crossing (yielding, transition from elastic to plastic behavior, etc.) happens before the melting, making the impression of melting (scenario B).

homogeneously. The temperature dependence is shown schematically by the lower curve in Fig. 9. There is also such a characteristic of the sample as yielding strength (or it could be elastoplastic limit) which decreases with temperature. These two effects have the same order of magnitude.[34,35] Two scenarios are possible. If the melting temperature is low, the yield strength and stress curves do not cross before the melting occurs (scenario A). If the melting temperature is high, those curves might cross before melting (scenario B). In the case of scenario A the true melting temperature is measured. In the case of B instead of melting temperature one might measure the temperature of yielding or beginning of plastic deformations. The change of absorption and surface motion will be observed in both scenarios. However, in case A, this is melting, in case B, this is not.

MgO is known to be a very soft material[36] and having a very high zero-pressure melting temperature. Therefore, if our explanation is a possible mechanism, then the first candidate where it should be true is MgO.

V. CONCLUSIONS

We have demonstrated that the good agreement in Ref. 2 between the MD calculated and measured in DAC LiF melting temperatures is partially due to incorrect calculations of melting temperatures. It is important to recognize that MD simulation of thermal instability has nothing in common with the simulation of melting and that these two features can be quite far from each other. Even though the Tosi-Fumi model is not capable of providing the absolute melting temperature of LiF, the model, corrected for application at high pressure, gives us a reasonable description of its pressure dependence with increasing pressure. The extrapolation of experimental melting temperatures derived from DAC are likely to be in agreement with shock-wave data if the extrapolation takes into account the possible $B1$-$B2$ transition in LiF. The transition was calculated to occur in the vicinity of 1 Mbar at the melting temperature, which is in accord with indirect evidence from shock-wave measurements and *ab initio* predictions. A model for LiF which would allow quantitative comparison of melting temperatures with experimental data has yet to be developed. One has to be careful when comparing theoretical and experimental melting curves—there is a possibility that what has been measured is not melting.

ACKNOWLEDGMENTS

A.B. is thankful to W. Smith for the DL_POLY software package. Discussion with R. Jeanloz was very informative. The help of the personal of the National Supercomputer Center in Linkoping is greatly appreciated. We wish to thank Swedish Research Council for Natural Sciences (NFR) and Swedish Materials Consortium 9 for financial support.

[1] Special issue of Philos. Trans. R. Soc. London, Ser. A **354**, 1 (1996).
[2] R. Boehler, M. Ross, and D.B. Boercker, Phys. Rev. Lett. **78**, 4589 (1997).
[3] L. Vocadlo and G.D. Price, Phys. Chem. Miner. **23**, 42 (1996).
[4] J.W.E. Lewis, K. Singer, and L.V. Woodcock, J. Chem. Soc., Faraday Trans 1 **71**, 301 (1975).
[5] M. Ross (private communication).
[6] M.J.L. Sangster and M. Dixon, Adv. Phys. **25**, 247 (1976).
[7] R. Eggenhoffner, F.G. Fumi, and C.S.N. Murthy, J. Phys. Chem. Solids **43**, 583 (1982).
[8] A.B. Belonoshko and L.S. Dubrovinsky, Geochim. Cosmochim. Acta **59**, 1883 (1995).
[9] R.J. Rustad, D.A. Yuen, and F.J. Spera, Phys. Rev. A **42**, 2081 (1990).
[10] M.P. Tosi and F.G. Fumi, J. Phys. Chem. Solids **25**, 45 (1964).
[11] A.J. Dekker, in *Solid State Physics* (Macmillan London, 1965), pp. 117–128.
[12] J.D. Gale, J. Chem. Soc., Faraday Trans. 1 **93**, 629 (1997).
[13] T. Yagi, J. Phys. Chem. Solids **39**, 563 (1978).
[14] W.J. Carter, High Temp.-High Press. **5**, 313 (1973).
[15] J.M. Wills (unpublished); J.M. Wills and B.R. Cooper, Phys. Rev. B **36**, 3809 (1987); D.L. Price and B.R. Cooper, *ibid.* **39**, 4945 (1989).
[16] L. Hedin and B.I. Lundqvist, J. Phys. C **4**, 2064 (1971).
[17] O.K. Andersen, Phys. Rev. B **12**, 3060 (1975).
[18] H.L. Skriver, *The LMTO Method* (Springer, Berlin, 1984).
[19] D.J. Chadi and M.L. Cohen, Phys. Rev. B **8**, 5747 (1973); S. Froyen, *ibid.* **39**, 3168 (1989).
[20] M.P. Allen and D.J. Tildesley, *Computer Simulation of Liquids* (Clarendon, Oxford, 1987).
[21] T.R. Forester and W. Smith, The DL_POLY_2.0 User Manual (CCLRC, Daresbury Laboratory, Daresbury, Warrington, England, 1998).
[22] W.G. Hoover, Phys. Rev. A **31**, 1695 (1985).
[23] D. Fincham, Mol. Simul. **8**, 165 (1992).
[24] A.B. Belonoshko and L.S. Dubrovinsky, Am. Mineral. **81**, 303 (1996).
[25] A.B. Belonoshko, Geochim. Cosmochim. Acta **58**, 4039 (1994).
[26] A.B. Belonoshko, Phys. Chem. Miner. **25**, 138 (1998).
[27] R. Ahuja, A.B. Belonoshko, and B. Johansson, Phys. Rev. E **57**, 1673 (1998).
[28] A.B. Belonoshko, R. Ahuja, O. Eriksson, and B. Johansson, Phys. Rev. B **61**, 3838 (2000).
[29] G. Ciccotti, J. Jacucci, and I.R. McDonald, Phys. Rev. A **13**, 426 (1976).
[30] J.R. Morris, C.Z. Wang, K.M. Ho, and C.T. Chan, Phys. Rev. B **49**, 3109 (1994).
[31] C.E. Sims, G.D. Barrera, N.L. Allan, and W.C. Mackrodt, Phys. Rev. B **57**, 11 164 (1998).
[32] S.B. Kormer, Usp. Fiz. Nauk **94**, 641 (1968) [Sov. Phys. Usp. **11**, 229 (1968)].
[33] J. Akella, S.N. Vaidya, and G.C. Kennedy, Phys. Rev. **185**, 1135 (1969).
[34] A.B. Belonoshko and L.S. Dubrovinsky, Am. Mineral. **82**, 441 (1997).
[35] D.J. Weidner, Y. Wang, and M.T. Vaughan, Geophys. Res. Lett. **21**, 753 (1994).
[36] G. Serghiou, A. Zerr, and R. Boehler, Science **285**, 983 (1999).
[37] S.B. Kormer, M.V. Sinitsyn, G.A. Kirillov, and V.D. Urlin, Zh. Éksp. Teor. Fiz. **48**, 1033 (1965) [Sov. Phys. JETP **21**, 689 (1965)].
[38] A. Zerr and R. Boehler, Nature (London) **371**, 506 (1994).